Catalysis Today 170 (2011) 50–55

Contents lists available at ScienceDirect

Catalysis Today

journal homepage: www.elsevier.com/locate/cattod

Hydrogen generation from coupling reactions of sodium borohydride and aluminum powder with aqueous solution of cobalt chloride

Hong-Bin Dai, Guang-Lu Ma, Xiang-Dong Kang, Ping Wang*

Shenyang National Laboratory for Materials Science, Institute of Metal Research, Chinese Academy of Sciences, 72 Wenhua Road, Shenyang 110016, PR China

ARTICLE INFO

Article history:
Received 13 July 2010
Received in revised form 26 October 2010
Accepted 28 October 2010
Available online 4 December 2010

Keywords:
Hydrogen generation
Hydrolysis reaction
Sodium borohydride
Aluminum powder
Catalyst

ABSTRACT

On-demand hydrogen generation from the hydrolysis reactions of chemical hydrides has gained ever-increasing attention as a promising approach for providing mobile/portable hydrogen sources. In this paper, we report a new chemical hydrogen storage system that is composed of sodium borohydride ($NaBH_4$)/aluminum (Al)/sodium hydroxide (NaOH) solid powder mixture and aqueous solution of cobalt chloride ($CoCl_2$). Hydrogen generation can be readily controlled by regulating the contact of the aqueous solution with the solid powder mixture. In comparison with the conventional $NaBH_4/H_2O$ or Al/H_2O systems, the newly developed dual-solid-fuel system exhibits distinct advantages in hydrogen storage density, hydrogen generation rate and fuel conversion. Additionally, the dual-solid-fuel system shows satisfactory transient response. The factors influencing the hydrogen generation performance of the system were studied. The reaction by-products were characterized using powder X-ray diffraction and Fourier transform infrared spectroscopy techniques. Our study demonstrated a high-performance dual-solid-fuel hydrogen generation system, and may lay a foundation for developing practical hydrogen generators for mobile/portable applications.

1. Introduction

The widespread use of hydrogen as a clean alternative to fossil fuels is severely hampered by the lack of safe and efficient means for hydrogen storage. The past decades have witnessed numerous efforts in developing solid-state hydrogen storage materials/technologies. However, extensive studies of various interstitial metal hydrides, complex metal hydrides and physisorbents have led to no viable system that can reversibly store >5 wt.% hydrogen under conditions that are relevant to the practical operation of proton exchange membrane fuel cell (PEMFC) [1]. Recently, chemical hydrides have gained ever-increasing attention as an important alternative to the reversible approach [2,3]. In comparison with the reversible hydride materials, on-demand hydrogen generation (HG) from chemical hydrides in conjunction with off-board spent fuel regeneration appears to provide a more realistic solution for near-term hydrogen storage applications.

$$NaBH_4 + (2+x)H_2O \xrightarrow{\text{Catalyst}} NaBO_2 \cdot xH_2O + 4H_2 \uparrow + 210\,\text{kJ} \qquad (1)$$

Sodium borohydride ($NaBH_4$) is a representative chemical hydride. Its hydrolysis reaction following Eq. (1) (where x denotes the excess of water) can be significantly accelerated by using metal catalysts or acid promoters, and decelerated or even terminated by adding alkaline stabilizer. The alkaline-stabilized aqueous solution of $NaBH_4$, in combination with the supported catalysts, therefore constitutes a controlled HG system. $NaBH_4$-based hydrolysis systems possess a series of advantages that merit their potential applications as mobile or portable hydrogen sources, including satisfactory reaction controllability, mild operation temperature, safe fuel storability, negligible environmental impact and minimized pretreatment requirement prior to feeding PEMFC end-user [2,3]. In the past decade, numerous efforts have been directed towards the development of $NaBH_4$-based HG system, which resulted in significant progress in synthesis of high-performance catalyst [4–7], device design [5,8,9], and regeneration chemistry [10,11]. However, even with the aid of these technological advances, the $NaBH_4$-based hydrolysis system is still greatly limited in the vehicular applications. One major problem is the low hydrogen density, due primarily to the solubility limitations of $NaBH_4$ and sodium metaborate ($NaBO_2$) by-product in aqueous solution [12], as well as the "dead weight" H_2O which exists in the form of $NaBO_2{\cdot}xH_2O$. According to the thermodynamic modeling study by Shang and Chen [13], the "optimum" hydrolysis system containing 8.5 wt.% $NaBH_4$/5 wt.% NaOH at 25 °C gives a material-based hydrogen density of 1.8 wt.%. This is only 1/6 of the theoretical value (10.8 wt.%) that is generated from the stoichiometric hydrolysis reaction following Eq. (1) ($x = 0$). Another major drawback that limits the

---

* Corresponding author. Tel.: +86 24 2397 1622; fax: +86 24 2389 1320.
E-mail address: pingwang@imr.ac.cn (P. Wang).

0920-5861/$ – see front matter © 2010 Elsevier B.V. All rights reserved.
doi:10.1016/j.cattod.2010.10.094

practical application of $NaBH_4$ is its prohibitively high cost. The current price of commercial $NaBH_4$ gives rise to an equivalent hydrogen cost of around US$200 per kg H_2, nearly two orders of magnitude higher than the DOE's US$2–3 per kg H_2 goal [14]. Whereas cost reduction is expectable through technology innovation in regenerating borate back to borohydride, $NaBH_4$ is apparently disqualified as a competitive transportation fuel for the near-term application [15].

Quite recently, two strategies have been employed in developing energy- and cost-effective chemical hydrogen storage systems. One is to directly use chemical hydrides as solid fuel to overcome the solubility limitation. When hydrogen is needed, the aqueous solution of catalysts [16,17] or acids [18,19] is regulated to contact with the solid fuel. Alternatively, addition of water to the premixed mixture of solid fuel and catalyst was also practiced [17,20–22]. As a consequence of the reduced water amount, the newly developed systems possess much higher hydrogen density than the conventional hydrolysis system [16–22]. The other strategy is to use cheap materials, e.g. aluminum (Al) [23] or its alloys [24], as a water-splitting agent for generating hydrogen. Al reacts with water to generate hydrogen gas following Eq. (2) at ambient condition. Although the gravimetric hydrogen density is relatively low (with a theoretical value of 3.7 wt.%),

$$Al + 3H_2O \xrightarrow{NaOH} Al(OH)_3 \downarrow + 1.5H_2 \uparrow + 426.5\,kJ \qquad (2)$$

the resource abundance and the low cost of Al (US$2.4 per kg primary Al) make Al/H_2O system promising for hydrogen storage applications [25]. In the study of the Al/H_2O system, a central issue is how to solve the self-restraining problem that originates from the formation of a coherent and adherent oxide layer on the Al surface. A number of reaction-promoting approaches are under investigation to address this problem. It has been demonstrated that additions of hydroxides [26], metal oxides [27] or selected salts [28] can effectively disrupt the passivation layer. Alternatively, alloying Al with low melting point metals has proven an effective approach for inhibiting the formation of a coherent passivation layer [29,30].

In the present study, we employ a combination of the two strategies to develop a new HG system, which is composed of $NaBH_4$/Al/NaOH powder mixture and cobalt chloride ($CoCl_2$) aqueous solution. On-demand HG can be readily achieved by regulating the addition of $CoCl_2$ aqueous solution to the solid powder mixture. In comparison with the conventional $NaBH_4$- or Al-based systems, the newly developed dual-solid-fuel ($NaBH_4$ + Al) system exhibits significant advantages on HG rate and fuel conversion. Additionally, the dual-solid-fuel system shows favorable performance in terms of hydrogen density and transient response. The combination of these advantages makes the ($NaBH_4$ + Al)/H_2O system promising for mobile/portable hydrogen source applications.

2. Experimental

$NaBH_4$ (96% purity), Al powder (100–200 mesh, 99% purity), NaOH (98% purity) and hydrated cobalt chloride ($CoCl_2 \cdot 6H_2O$, 99% purity) were purchased from Sinopharm Chemical Reagent Corp. and used as received. Deionized water was used in preparation of all the aqueous solutions. The $NaBH_4$/Al/NaOH powder mixtures in varied mass ratios were hand-milled using agate mortar and pestle in an Ar (99.999%)-filled glove box.

Fig. 1 presents a schematic diagram of the experimental setup used for the measurement of HG properties. The catalytic hydrolysis reaction was carried out in a 250 mL three-neck flask, wherein the precisely weighed solid fuel was preloaded. A $CoCl_2$ aqueous solution with desired concentration was fed into contact with the solid fuel in the reactor using a pressure-equalizing dropping funnel. Typically, the dropping rate of the aqueous solution was controlled at around 3 g min^{-1}, which ensures a reliable comparison of the HG dynamics of different systems. The generated hydrogen gas passed through a heat exchanger to cool to room temperature followed by contacting with a silica drier to remove water vapor. The HG rate was measured using an online mass flow meter (Sevenstar Huachang, MFM D07–7BM, accuracy within ±2%) that was equipped with a computer. The HG volume was calculated by integrating the measured HG rate over time. The reaction temperature was monitored using a thermocouple embedded in the solid fuel bed and recorded using an online recorder. For each solid fuel composition, the experiment was repeated two times. The determined relative error was no more than ±3%.

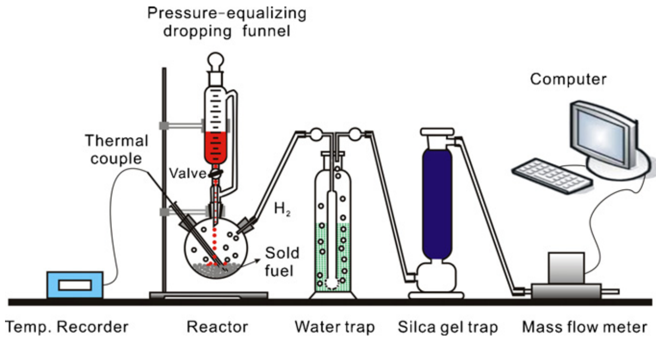

Fig. 1. Schematic diagram of experimental setup.

The solid by-products of the hydrolysis reaction were analyzed by powder X-ray diffraction (PXRD, Rigaku D/MAX-2500, Cu Kα radiation) and Fourier transform infrared spectroscopy (FTIR, Bruker TENSOR 27, MCT detector). Elemental analysis was performed using inductively coupled plasma-atomic emission spectrometry (ICP-AES, Iris Intrepid).

3. Results and discussion

3.1. Hydrogen generation dynamics

Both $NaBH_4$ and Al (or its alloys) have been extensively studied as potential fuel for HG. In the present study, we constituted a new HG system that was composed of $NaBH_4$/Al/NaOH powder mixture and $CoCl_2$ solution. The NaOH additive acts to disrupt the aluminum oxide (Al_2O_3) layer on the Al surface following Eq. (3). Its addition amount varied with Al amount, but with the NaOH: Al mass ratio fixed at 1:5.

$$Al_2O_3 + 2NaOH + 3H_2O \rightarrow 2NaAl(OH)_4 \qquad (3)$$

The selection of $CoCl_2$ as a catalyst is based on its well established promoting effect on the hydrolysis reaction of $NaBH_4$ [31,32]. According to Levy et al. [32], $CoCl_2$ aqueous solution reacts with $NaBH_4$ following Eq. (4), resulting in the formation of catalytically active Co_2B, which appears as a black precipitate in the aqueous solution.

$$CoCl_2 + 2NaBH_4 + 3H_2O \rightarrow 0.5Co_2B \downarrow + 2NaCl + 1.5HBO_2 + 6.25H_2 \uparrow \qquad (4)$$

As shown in Fig. 2(a), contact of aqueous solution of $CoCl_2$ with $NaBH_4$/Al/NaOH powder mixture initiates rapid hydrogen release. The system reached its maximum HG rate of 4.8 L min^{-1} after a duration of around 0.5 min, and completed ∼90% fuel conversion after 3 min. As the exothermic reaction proceeded, the temperature of the fuel slurry promptly increased to around 100 °C, followed by a gradual temperature decrease. The elevated system temper-

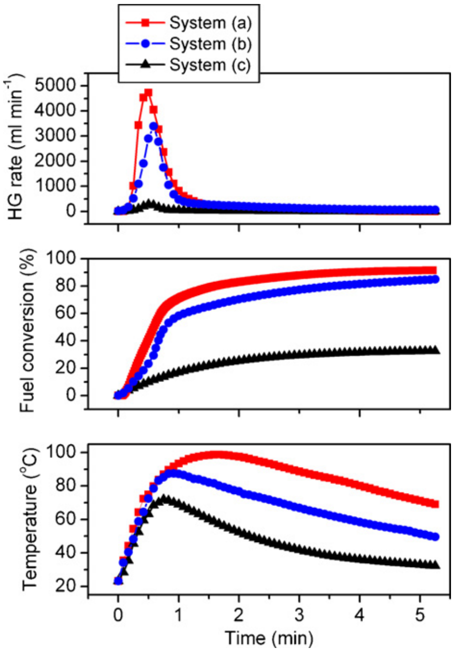

Fig. 2. A comparison of HG rate (top), fuel conversion (middle) and system temperature (bottom) among the systems. (a) 1.0 g of $NaBH_4$, 0.5 g of Al powder, 0.1 g of NaOH and 3 g of 5 wt.% $CoCl_2$ aqueous solution; (b) 1.0 g of $NaBH_4$, 0.1 g of NaOH and 2.0 g of 7.5 wt.% $CoCl_2$ solution; (c) 0.5 g of Al powder, 0.1 g of NaOH and 1.0 g of 5 wt.% $CoCl_2$ solution.

ature causes water evaporation, which makes the water supply deficient to react with the solid fuel. This is one possible reason for the incomplete fuel conversion.

For comparison, the corresponding results of the systems containing individual $NaBH_4$ or Al solid fuel are included in Fig. 2(b) and (c), respectively. It was found that, even with the presence of NaOH stabilizer, addition of $CoCl_2$ solution can significantly accelerate the hydrolysis reaction of $NaBH_4$ ($NaBH_4$:NaOH = 10:1, the addition of NaOH is to improve the storability of $NaBH_4$ solid fuel and to ensure a reliable property comparison). Here, to ensure the same catalyst content in the two systems, the $CoCl_2$ concentration in the $NaBH_4$-based system was increased to 7.5 wt.%. It was found that the HG rate of the $NaBH_4$ system is significantly lower than that of the $NaBH_4$ + Al dual-solid-fuel system. Among the three systems examined, the Al/H_2O reaction system shows the worst HG performance. Only at the initial stage does the Al/H_2O reaction system show an appreciable HG rate, with a maximum value of 482 mL min^{-1}. After 2.5 min, the Al/H_2O reaction largely terminated, resulting in a fuel conversion of only 34%. Evidently, it is the surface passivation that inhibits the Al/H_2O reaction, indicating that the applied alkaline concentration is insufficient for disrupting the in situ reformed passivation layer on the surface of Al powder.

Comparison of the HG performances of the three systems clearly indicates that the dual-solid-fuel system involves a synergetic promoting mechanism [24]. Fundamentally, it should be understood from the coupling effects of the following aspects: the catalytic hydrolysis of $NaBH_4$ results in elevated alkalinity of the aqueous solution [31], and thereby promoting the Al/H_2O reaction through disrupting the passivation layer. As the highly exothermic Al/H_2O reaction proceeds, the solution temperature is further increased, which in turn promotes the hydrolysis reaction of $NaBH_4$. In addition, the in situ formed Co_2B fine particles may play dual roles in the HG process. Besides its catalytic effect on the hydrolysis reaction of $NaBH_4$, Co_2B particles may deposit on the Al powder surface and function as a cathode of a micro-galvanic couple. This will reduce the hydrogen overpotential, thereby accelerating the corrosion of metallic Al [33]. Currently, the detailed studies are still ongoing to further the mechanistic understanding of the HG process of the ($NaBH_4$ + Al)/H_2O system.

The HG performance of the ($NaBH_4$ + Al)/H_2O system was found to be highly dependent on the system composition. In an effort to optimize the system composition, we firstly examined the effect of the solid fuel component ratios on the HG performance of the system. Table 1 summarizes the hydrogen densities and fuel conversions of the systems with varied Al and $NaBH_4$ mass ratios. Partial substitution of $NaBH_4$ by Al results in a decrease of the theoretical hydrogen density of the system, owing to the low hydrogen density of the Al/H_2O reaction system. But on the other hand, partial replacement of $NaBH_4$ by Al powder was found to exert a positive effect on the fuel conversion under the applied experimental conditions. This, to a certain extent, compensates for the hydrogen capacity loss. For the systems containing 25–50 wt.% Al powder relative to the total weight of $NaBH_4$ + Al mixture, the material-based hydrogen densities ranging from 5.8 to 4.9 wt.% has been experimentally demonstrated. Here, the hydrogen densities were determined on the basis of the total weights of the solid and liquid fuels. In an overall consideration of hydrogen density, fuel conversion and material cost, we selected the solid fuel with a mass ratio of Al:$NaBH_4$ = 1:2 for further investigation.

Next, we examined the effect of catalyst amount on the HG performance of the system. Fig. 3 presents the HG kinetic curves of the systems composed of 1 g of $NaBH_4$, 0.5 g of Al, 0.1 g of NaOH, and 3 g of aqueous solution of $CoCl_2$. The sole variable in the set of experiments is the $CoCl_2$ concentration in the aqueous solution. As expected, increasing the $CoCl_2$ concentration results in increasingly pronounced improvement on the HG kinetics, as well as the elimination of the induction period that was observed in the system without catalyst. For the system using a 5 wt.% $CoCl_2$ aqueous solution, 90% fuel conversion was accomplished within 3 min. When the

Table 1
Theoretical and experimental hydrogen densities and fuel conversions of the ($NaBH_4$ + Al)/H_2O systems containing different solid fuel component.

Al:$NaBH_4$ (mass ratio)	Al/(Al+$NaBH_4$) (wt.%)	Hydrogen density (wt.%)		Fuel conversion (%)
		Theoretical	Experimental	
0:1	0	7.2	6.2	86
1:3	25	6.2	5.8	93
1:2	33	5.9	5.4	91
1:1.5	40	5.6	5.2	92
1:1	50	5.3	4.9	93
1.5:1	60	4.9	4.4	90
2:1	67	4.6	4.2	91
3:1	75	4.3	3.8	89
1:0	100	3.5	1.2	34

Note: (a) The mass of water required to fully react with the solid fuels following Eqs. (1) (x = 2) and (2), respectively, and the theoretical hydrogen amounts are as follows: 1 g $NaBH_4$ ~ 1.9 g $H_2O \rightarrow$ 0.21 g H_2 (2.37 L, STP), 1 g Al ~ 2 g $H_2O \rightarrow$ 0.11 g H_2 (1.24 L, STP). (b) The mass ratio of solid and liquid fuels is 1:2 for all the systems, the mass ratio of Al and NaOH is 5:1, $CoCl_2$ concentration is fixed at 5 wt.%.

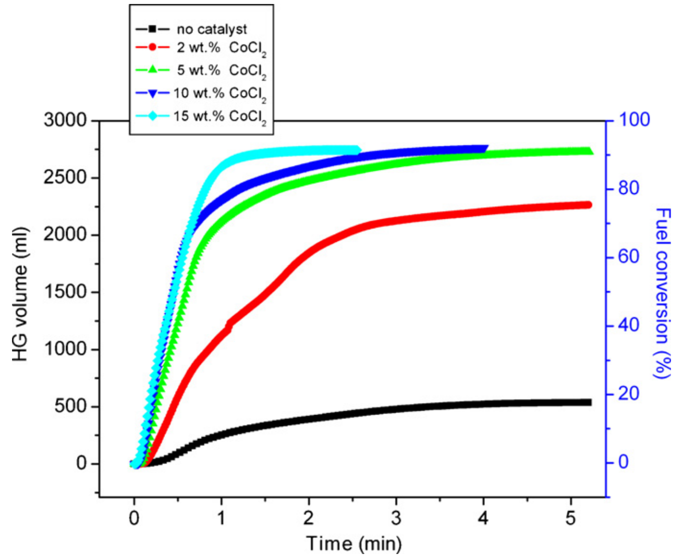

Fig. 3. Effects of $CoCl_2$ concentration on the HG volume and fuel conversion of the system composed of 1.0 g of $NaBH_4$, 0.5 g of Al powder, 0.1 g of NaOH and 3 g of $CoCl_2$ aqueous solution.

$CoCl_2$ concentration was increased to 15 wt.%, the system largely completed the HG within 1.5 min. However, increased catalyst concentration does not give rise to further increase of fuel conversion. A similar observation was also reported by Zhang and Mohring in their study of H_2SO_4-catalyzed hydrolysis of solid $NaBH_4$ system [19]. Presumably, this should be ascribed to a mass-transfer-limited phenomenon that is associated with the insufficient water supply. Additionally, the foaming by-products become the predominant constituent of the system at the late reaction stage, which may accumulate on the solid fuel powder surface and block the contact of the unreacted solid fuel with the residual water.

In the $(NaBH_4 + Al)/H_2O$ system, high fuel conversion is achievable through moderately increasing the water supply. As shown in the top of Fig. 4, a 100% fuel conversion was achieved when the amount of 5 wt.% $CoCl_2$ aqueous solution was increased to over 5 g. But meanwhile, increased water supply results in a decrease of hydrogen density of the system, as seen in the bottom of Fig. 4. An overall consideration of fuel conversion and hydrogen density suggests that, for the $NaBH_4 + Al$ solid fuel in a 2:1 mass ratio, a doubled water supply of the mass of solid fuel is optimum. As seen in Table 2, thus-constituted system possesses a favorable combination of high hydrogen density (5.4 wt.%), high fuel conversion (over 90%) and rapid HG dynamics (4.8 L min^{-1}), which are comparable to the best performances of $NaBH_4$-based HG systems, and much better than those of Al-based HG systems. Importantly, the $NaBH_4 + Al$ dual-solid-fuel system shows advantage over $NaBH_4$-based systems on the hydrogen production cost, which benefits its potential applications.

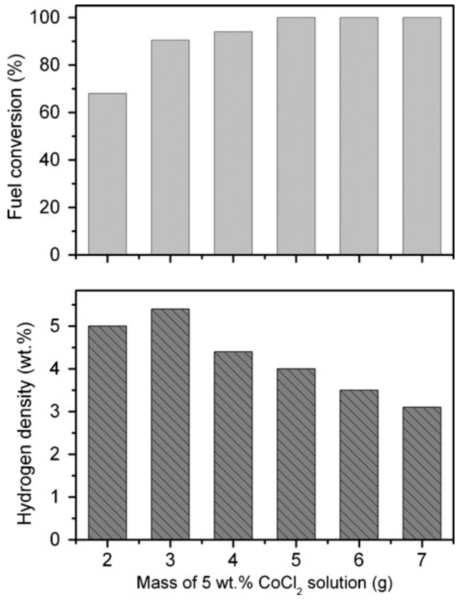

Fig. 4. Effects of water amount on fuel conversion (top) and hydrogen density (bottom) of the system composed of 1.0 g of $NaBH_4$, 0.5 g of Al powder and 0.1 g of NaOH. The $CoCl_2$ concentration was fixed at 5 wt.%.

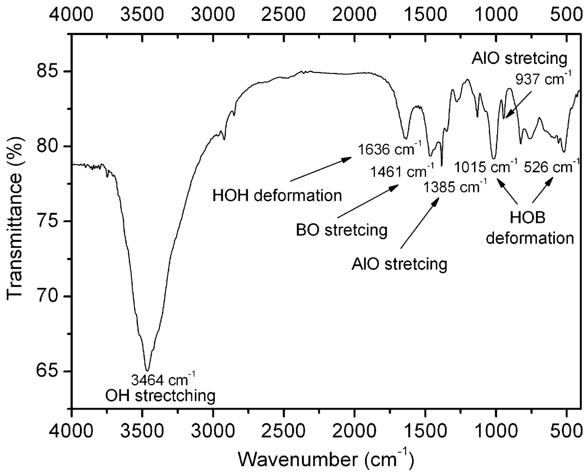

Fig. 5. FTIR spectrum of the reaction by-products. The HG system is composed of 1.0 g of $NaBH_4$, 0.5 g of Al powder, 0.1 g of NaOH, and 3 g of 5 wt.% $CoCl_2$ aqueous solution.

3.2. *By-products analysis*

The system composed of 1 g of $NaBH_4$, 0.5 g of Al, 0.1 g of NaOH, and 3 g of 5 wt.% $CoCl_2$ aqueous solution was selected for by-products analysis. The by-products of the reactions were collected and dried under vacuum at 75 °C for 24 h. The obtained grey solid powder was characterized by FTIR. As shown in Fig. 5, the characteristic B–O, Al–O stretching bands were clearly identified in the region of 900–1500 cm^{-1}, indicative of the formation of B–O, Al–O compounds [34]. As expected, the O–H stretching, H–O–H deformation and H–O–B deformation bands were also identified, which is consistent with the formation of hydrated by-products. Additionally, it was noticed that the characteristic B–H stretching band of $NaBH_4$ at 2280 cm^{-1} completely disappeared in the IR spectrum [10]. This finding suggests that the residual solid fuel that is responsible for the 90% conversion should be predominantly Al powder.

Fig. 6 presents the XRD pattern of the reaction byproducts. As expected, $NaBO_2{\cdot}2H_2O$ (JCPDF card 06–0122) and $Al(OH)_3$ (JCPDF card 15–0136) were identified as the major by-products of the hydrolysis reaction of $NaBH_4$ and the Al/H_2O reaction, respectively. Additionally, the XRD pattern shows the presence of small amounts of $NaBO_2{\cdot}4H_2O$ (JCPDF card 20–1078), $Na_2B_4O_7$ (JCPDF card 15–0136), $NaOH{\cdot}H_2O$ (JCPDF card 30–1194), and $Na_2CO_3{\cdot}10H_2O$ (JCPDF card 01–0938) by-products. Here, the crystalline $Na_2B_4O_7$ and $Na_2CO_3{\cdot}10H_2O$ were not generated in the hydrolysis reaction, but they are the products from the reactions of the $NaBO_2$ by-product and NaOH stabilizer with CO_2 in air following Eqs. (5) and (6), respectively [16]. Na_2CO_3 subsequently hydrated with H_2O to form $Na_2CO_3{\cdot}10H_2O$. Notably, no diffraction peak of Al was identified in the XRD pattern, whereas its presence is sug-

Table 2
A comparison of hydrogen generation performances of the NaBH4 + Al dual-solid-fuel system and the relevant single-solid-fuel systems.

Systems	Materials and operating conditions	HG rate ($L\,min^{-1}$)	Fuel conversion (%)	Hydrogen density (wt.%)	Ref.
$NaBH_4/Al/H_2O$	1.0 g $NaBH_4$(s)/0.5 g Al/0.10 g NaOH/3.0 g 5 wt.% $CoCl_2$ solution, 0.1 MPa	4.8	91	5.4	This paper
$NaBH_4/H_2O$	1.0 g $NaBH_4$(s)/0.10 g NaOH/2.0 g 7.5 wt.% $CoCl_2$ solution, 0.1 MPa	3.5	86	6.2	This paper
	1.02 g $NaBH_4$(s)/0.2 g $CoCl_2$/1.5 g H_2O, 0.1 MPa	–	81.2	6.7	[16]
	1.14 g $NaBH_4$(s)/0.14 g Co^{2+}–IR120/2.0 g H_2O, 0.1 MPa	0.67	91	6.7	[20]
	1.2 g $NaBH_4$(s)/0.48 g Ni–Ru/2.3 g H_2O, 1.26 MPa	11.6	98	6.3	[22]
Al/H_2O	0.5 g Al/0.1g NaOH/1.0 g H_2O, 0.1 MPa	0.48	34	1.2	This paper
	0.20 g 30 vol% Al–70 vol% γ-Al_2O_3/270 g H_2O at 22 °C, 0.1 MPa	1.3×10^{-3}	100	–	[27]
	1.0 g Al–10 wt.%Bi–5 wt.% NaCl alloy/10 g H_2O, 0.1 MPa	0.53	85.4	–	[30]
	0.2 g Al/75 mL 0.1 M Na_2SnO_3 at 75 °C, 0.1 MPa	0.24	71	–	[34]

gested by the combination of the HG property examination and FTIR results. Most probably, the invisibility of crystalline Al in the XRD analysis originates from its "encapsulation" by the accumulated by-products. In this regard, detailed microstructural studies may provide conclusive evidence.

$$4NaBO_2 + CO_2 \rightarrow Na_2B_4O_7 + Na_2CO_3 \quad (5)$$

$$NaOH + CO_2 \rightarrow Na_2CO_3 + H_2O \quad (6)$$

In the present study, $CoCl_2$ was used as a catalyst. But the XRD examination of the reaction by-products cannot detect any Co-containing crystalline phase. In an effort to characterize the catalytically active species, we treated the by-products by using magnetic separation technique and examined the separated material by XRD and elemental analysis. As shown in Fig. 6(b), the separated black powder possesses an amorphous structure. Quantitative elemental analysis by using ICP-AES determined that the material is composed of 91.3 wt.% Co and 8.7 wt.% B, corresponding to a formula of $Co_{1.93}B$. These results agree well with the early observation of Schlesinger et al. [31].

3.3. *"Start–stop" hydrogen generation dynamics*

Transient response is a key aspect in evaluating the performance of a practical hydrogen generator. In the present system, $CoCl_2$ aqueous solution was used as a HG controlling agent. The transient response property was examined by measuring a discontinuous HG process that involved repetitious start/stop of the addition of $CoCl_2$ aqueous solution. As shown in Fig. 7, instantaneous HG was initiated upon contacting the $NaBH_4$ + Al solid fuel with $CoCl_2$ aqueous solution. After switching off the $CoCl_2$ aqueous solution supply, the HG reactions can be terminated within about 5 min. Repetitious switch on/off the $CoCl_2$ aqueous solution supply was found to exert appreciable effect on the maximum HG rate and the time duration to reach it. For example, the maximum HG rate at the third cycle is around 20% lower than that at the first cycle. One possible reason for this property degradation might come from the accumulated by-products on the surface of the unreacted solid $NaBH_4$ and Al powder that block the liquid fuel from contacting the solid fuel. The ($NaBH_4$ + Al)/H_2O system exhibits satisfactory transient response. This is of significance for the practical design of a hydrogen generator, as it allows for a smaller ballast tank size, thus giving rise to an increased hydrogen density on the system basis.

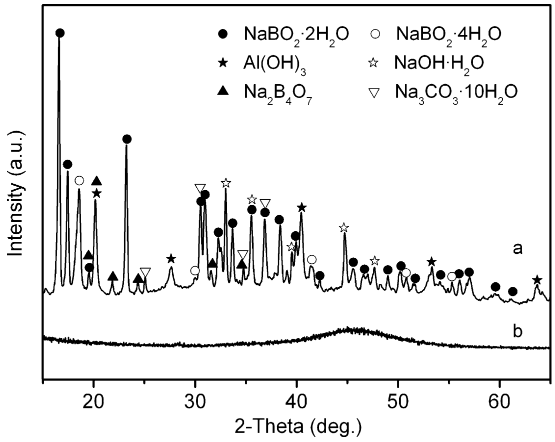

Fig. 6. (a) XRD pattern of the reaction by-products of the system composed of 1.0 g of $NaBH_4$, 0.5 g of Al powder, 0.1 g of NaOH, and 3 g of 5 wt.% $CoCl_2$ aqueous solution; (b) XRD pattern of the substance that was separated from the reaction by-products using magnetic separation technique.

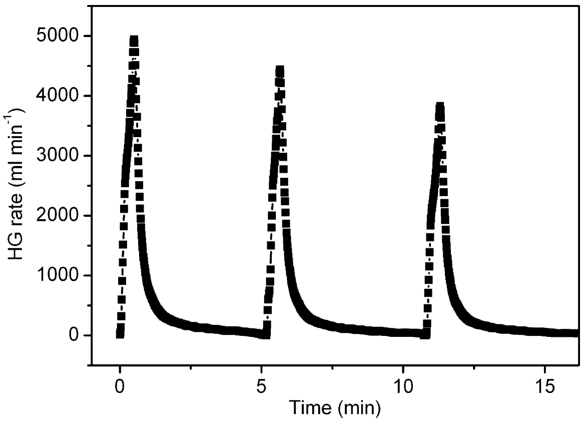

Fig. 7. "Start/stop" HG dynamics profile of the ($NaBH_4$ + Al)/H_2O system.

4. Conclusions

Our study demonstrated that $NaBH_4$/Al/NaOH solid powder mixture, in combination with the aqueous solution of $CoCl_2$, constitutes a high-performance hydrogen generation system. As a consequence of the mutual-promoting effects of the hydrolysis reaction of $NaBH_4$ and the Al/H_2O reaction, the dual-solid-fuel system exhibits the significant advantages over the conventional $NaBH_4/H_2O$ or Al/H_2O reaction systems in terms of hydrogen density, hydrogen generation rate and fuel conversion. A preliminary investigation has elucidated the effects of solid fuel component ratios, catalyst concentration and water amount on the hydrogen generation performance of the system. With an optimized fuel composition, the system can achieve over 90% fuel conversion within 5 min, giving rise to a material-based hydrogen density of 5.4 wt.%. The favorable combination of high hydrogen density, high hydrogen generation rate, satisfactory fuel conversion at ambient temperatures and prompt transient response makes the ($NaBH_4 + Al$)/H_2O system very promising for mobile/portable hydrogen source applications. Furthermore, our study shows the feasibility of achieving high-performance hydrogen generation using cheap material, thereby laying a foundation for developing practical hydrogen generators.

Acknowledgements

The financial supports for this research from the National High-Tech. R&D Program of China (863 Program, 2009AA05Z109), the National Basic Research Program of China (973 program, 2010CB631305), the National Natural Science Foundation of China (51071155) and the Frontier Project of CAS Knowledge Innovation Program (KGCXZ-YW-342) are gratefully acknowledged.

References

[1] U. Eberle, M. Felderhoff, F. Schüth, Angew. Chem. Int. Ed. 48 (2009) 6608.
[2] P. Wang, X.D. Kang, Dalton Trans. 40 (2008) 5400.
[3] U.B. Demirci, O. Akdim, J. Andrieux, J. Hannauer, R. Chamoun, P. Miele, Fuel Cells 10 (2010) 335.
[4] S.C. Amendola, S.L. Sharp-Goldman, M.S. Janjua, M.T. Kelly, P.J. Petillo, M. Binder, J. Power Sources 85 (2000) 186.
[5] Y. Kojima, K. Suzuki, K. Fukumoto, Y. Kawai, M. Kimbara, H. Nakanishi, S. Matsumoto, J. Power Sources 125 (2004) 22.
[6] H.B. Dai, Y. Liang, P. Wang, X.D. Yao, T. Rufford, M. Lu, H.M. Cheng, Int. J. Hydrogen Energy 33 (2008) 4405.
[7] N. Patel, R. Fernandes, A. Miotello, J. Catal. 271 (2010) 315.
[8] Q. Zhang, G. Smith, Y. Wu, R. Mohring, Int. J. Hydrogen Energy 31 (2006) 961.
[9] A. Pozio, M. De Francesco, G. Monteleone, R. Oronzio, S. Galli, C. D'Angelo, M. Marrucci, Int. J. Hydrogen Energy 33 (2008) 51.
[10] Y. Kojima, T. Haga, Int. J. Hydrogen Energy 28 (2003) 989.
[11] H. Zhang, S. Zheng, F. Fang, G. Chen, G. Sang, D. Sun, J. Alloys Compd. 484 (2009) 352.
[12] U.B. Demirci, O. Akdim, P. Miele, Int. J. Hydrogen Energy 34 (2009) 2638.
[13] Y. Shang, R. Chen, Energy Fuels 20 (2006) 2142.
[14] O.A. Moreno, M.T. Kelly, J.V. Ortega, DOE Hydrogen Program FY 2007 Annual Progress Report, 2007, http://www.hydrogen.energy.gov/pdfs/progress07/iv_b_2_moreno.pdf.
[15] Go/no-go recommendation for sodium borohydride for on-board vehicular hydrogen storage, U.S. Department of Energy Hydrogen Program, Independent Review, November 2007. http://www.hydrogen.energy.gov/pdfs/42220.pdf.
[16] B.H. Liu, Z.P. Li, S. Suda, J. Alloys Compd. 468 (2009) 493.
[17] P. Gislon, G. Monteleone, P.P. Prosini, Int. J. Hydrogen Energy 34 (2009) 929.
[18] O. Akdim, U.B. Demirci, P. Miele, Int. J. Hydrogen Energy 34 (2009) 7231.
[19] Q. Zhang, R.M. Mohring, Ind. Eng. Chem. Res. 48 (2009) 1603.
[20] C.H. Liu, Y.C. Kuo, B.H. Chen, C.L. Hsueh, K.J. Hwang, J.R. Ku, F. Tsau, M.S. Jeng, Int. J. Hydrogen Energy 35 (2010) 4027.
[21] C.H. Liu, B.H. Chen, C.L. Hsueh, J.R. Ku, F. Tsau, J. Power Sources 195 (2010) 3887.
[22] M.J.F. Ferreira, L. Gales, V.R. Fernandes, C.M. Rangel, A.M.F.R. Pinto, Int. J. Hydrogen Energy 35 (2010) 9869.
[23] E. Shafirovich, V. Diakov, A. Varma, Combust. Flame 144 (2006) 415.
[24] L. Soler, J. Macanás, M. Muñoz, J. Casado, Int. J. Hydrogen Energy 32 (2007) 4702.
[25] H.Z. Wang, D.Y.C. Leung, M.K.H. Leung, M. Ni, Renew. Sust. Energy Rev. 13 (2009) 845.
[26] L. Soler, J. Macanás, M. Muñoz, J. Casado, J. Power Sources 169 (2007) 144.
[27] Z.Y. Deng, Y.B. Tang, L.L. Zhu, Y. Sakka, J. Ye, Int. J. Hydrogen Energy 35 (2010) 9561.
[28] J. Skrovan, A. Alfantazi, T. Troczynski, J. Appl. Electrochem. 39 (2009) 1695.
[29] W. Wang, D.M. Chen, K. Yang, Int. J. Hydrogen Energy 35 (2010) 12011.
[30] M.Q. Fan, L.X. Sun, F. Xu, Energy 35 (2010) 2922.
[31] H.I. Schlesinger, H.C. Brown, A.E. Finholt, J.R. Gilbreath, H.R. Hoekstra, E.K. Hyde, J. Am. Chem. Soc. 75 (1953) 215.
[32] A. Levy, J.B. Brown, C.J. Lyons, Ind. Eng. Chem. 52 (1960) 211.
[33] L. Soler, A.M. Candela, J. Macanás, M. Muñoz, J. Casado, Int. J. Hydrogen. Energy 35 (2010) 1038.
[34] U.B. Demirci, O. Akdim, P. Miele, J. Power Sources 192 (2009) 310.